Original scientific paper

POSSIBILISTIC UNCERTAINTY ASSESSMENT IN THE PRESENCE OF OPTIMALLY INTEGRATED SOLAR PV-DG AND PROBABILISTIC LOAD MODEL IN DISTRIBUTION NETWORK

Shradha Singh Parihar, Nitin Malik

The NorthCap University, Gurgaon, India

Abstract. *To integrate network load and line uncertainties in the radial distribution network (RDN), the probabilistic and possibilistic method has been applied. The load uncertainty is considered to vary as Gaussian distribution function whereas line uncertainty is varied at a fixed proportion. A voltage stability index is proposed to assign solar PV-DG optimally followed by application of PSO technique to determine the optimal power rating of DG. Standard IEEE 33- and 69-bus RDN are considered for the analysis. The impact of various uncertainties in the presence of optimally integrated solar PV-DG has been carried out on 69-bus network. The results obtained are superior to fuzzy-arithmetic algorithm. Faster convergence characteristic is obtained and analyzed at different degree of belongingness and realistic load models. The narrower interval width indicates that the observed results are numerically stable. To improve network performance, the technique takes into account long-term changes in the load profile during the planning stage. The significant drop in network power losses, upgraded bus voltage profile and noteworthy energy loss savings are observed due to the introduction of renewable DG. The results are also statistically verified.*

Key words: *distribution network, distributed generation, optimal integration, uncertainties, Interval arithmetic, Gaussian distribution function*

1. INTRODUCTION

1.1. Motivation and Literature review

The distribution network is ill-conditioned because of low X/R ratio and its radial structure. Thus, the conventional approaches like Newton-Raphson, Gauss-seidel, etc, for solving power flow (PF) problem in the transmission network fails to converge in many cases in distribution network. To compute bus voltage and power flow values, deterministic PF algorithm requires precise network (N/w) load and generation data. It does not

contribute to optimal planning and operation of the N/w, as it finds the PF results for specific N/w configuration and operating conditions only at a given instant. The emphasis is on integrating distributed generation (DG) into the distribution N/w due to socioeconomic, environmental, and technical constraints. DG is a decentralized generation of electric power in distribution N/w using non-renewable (turbine, engine, etc.) or renewable (small/micro/mini hydropower, wind, solar, fuel cell, geothermal, etc.) resources. As the output of these technologies depicts stochastic behavior, hence, capable to introduce significant uncertainty in total power production.

In real, the networks are complex due to the presence of non-linearity and incapability in expressing N/w variables in very precise terms which can be simplified by either allowing some degree of uncertainty or making assumptions about the distribution N/w. The input parameters (N/w load, line, and transformer data) are considered to be fixed while performing power grid operations, however they are not in practise. Because of the erroneous calculation of reactance and resistance due to conductor ageing and temperature variation, there is ambiguity in N/w line data. The load uncertainties are caused due to incorrect estimation in load demand (load forecasting). Changes in climate and water runoff induce uncertainty in hydropower plants. Temperature sensitivity in a fuel cell creates uncertainty since temperature change has a stronger impact at higher current [1]. This varies the power flow in the radial distribution network (RDN).

These uncertainties are modeled either using a possibilistic or probabilistic method. Monte Carlo simulation (MCS) and stochastic approach belongs to probabilistic domain whereas Interval Arithmetic (IA) and fuzzy sets comes under possibilistic methods. IA establishes a strict constraint on all feasible N/w circumstances that could have been achieved by hundreds of successive MCS; as a result, the MCS calculation time increases, making analysis more difficult. With little computational effort, IA can produce high-quality results.

Probabilistic and possibilistic modelling is quantitative and qualitative in nature, respectively [2]. Probabilistic method is used where sufficient historical data of uncertain parameter or their probability density function (PDF) like load pattern, wind speed and solar irradiation [3] is easily available whereas possibilistic modelling is preferred when the data available is not sufficient for the planners and operators to establish PDF [3]. Both the methods are cooperative and their utilization provides more realistic approximation to N/w modelling.

The approaches for integrating DG are generally categorized as analytical and heuristic methods. The analytical method makes use of mathematical equations to determine the optimum solution. An analytical method for evaluating DG in N/w is presented in [4] without considering cost benefits. Many numerical approaches like Kalman filter algorithm [5] and mixed integer non-linear programming [6] are applied to integrate DG optimally in the RDN. Authors in [7], demonstrated an analytical and a meta-heuristic approach to optimally allocate DG units in the RDN. Numerous evolutionary algorithms such as Grey Wolf Optimizer [8], PSO [9] and gravitational search algorithm [10] and have been employed for solving issues related to DG allocation in the RDN. An ant lion optimization algorithm [11] is demonstrated to optimally allocate DG in the RDN. Authors in [12], utilized augmented Lagrangian genetic algorithm to integrate renewable DGs for minimizing N/w losses, satisfying operational constraints without considering economic benefits.

In [13], author implements an IA technique to incorporate load uncertainty in the distribution N/w considering constant power load only. A correlated interval-based

backward/forward (b/f) PF method is developed in [14] to consider uncertainties in renewable energy resources. The interval-based PF models are transformed into the optimization problem in [15] which minimizes the conservatism of the obtained interval solutions. An Affine Arithmetic method is projected in [16] to introduce N/w uncertainties of different types. A probabilistic distribution-based IA approach is presented in [17] to introduce uncertainty in load demand in conventional PF. Authors in [18], demonstrated the IA based PF analysis in the presence of load, line and DG uncertainties. The analysis has also been done with various types of DG units that are not optimally allocated. Abdelkader et al. [19] proposed a Fuzzy Arithmetic Algorithm (FAA) for incorporating uncertainties in the RDN. Triangular fuzzy number method is proposed in [20] to introduce uncertainties in the N/w but resulted in higher N/w loss. To deal with N/w uncertainties a new midpoint-radius interval-based approach has been demonstrated in [21] to eliminate the factorization of the interval Jacobian matrix.

1.2. Paper contributions

From the previously published literature, it has been concluded that the combined use of the Interval Arithmetic and probabilistic load model with optimally integrated solar photovoltaic (PV) DG in distribution N/w has not been explored before. Using the hybrid possibilistic-probabilistic strategy, this research article contributes to the published literature. The optimal penetration of solar PV-DG is carried out using a novel voltage stability index (VSI) and PSO method and, thereafter, the N/w uncertainties (line and load) are introduced in RDN to demonstrate the possible states of the solution. The detailed investigation considering various realistic loads and load fluctuations with and without solar PV-DG have been presented. The presented approach is applied on well-established standard IEEE 69-bus N/w. Two case studies considering solar PV-DG without and with N/w uncertainties are analysed and the results of the IEEE 33-bus N/w are further compared to FAA to establish the effectiveness of the proposed methodology. The summarized article contributions are mentioned below

a) A new VSI has been developed for the optimal placement of solar PV-DG in a RDN after which PSO is implemented to find the optimal size of DG. This independent method for integrating renewable DG gives openness and versatility to the problem.

b) A combination of IA and probabilistic load model is applied and presented to attain a more realistic representation of distribution N/w modelling which paves the way for accurate results.

c) All input variables (loads and line) and generation in the distribution N/w are represented as random variables. The line uncertainty variables are considered to fluctuate at a constant proportion, whereas load uncertainty is expected to change according to a Gaussian distribution function.

d) The effect of N/w uncertainties and different realistic loads (industrial, residential and commercial) and their combination with optimally integrated solar PV-DG is analysed by directly incorporating them into the Interval-based b/f PF algorithm.

e) The analysis of the reduction in N/w losses and the cost of annual energy loss savings (AELS) has been carried out at three load levels to aid the distribution N/w operators (DNOs) in future N/w planning.

f) The attained results of the simulation study imply that the methodology proposed in this research is much more feasible and effective for designing the large-scale RDN at all load levels.

1.3. Paper outline

The brief outline of the work is given as: In Section 2, the description of Interval Arithmetic is mentioned. In section 3, the modeling of N/w data and DG is presented. In the next section, the working of the PSO is explained. Section 5 explores the development of the novel VSI and the algorithm to integrate solar PV-DG optimally in the N/w. Interval-based b/f PF solution is attained in Section 6. The simulated results for two standard RDN are mentioned in Section 7 followed by conclusion in last section.

2. INTERVAL ARITHMETIC

In contrast to the point estimating technique, a number can be expressed as confidence interval that can be open, closed, or a combination of both in the IA approach. A set of real numbers can be used to express an interval number. Let L and K be two separate interval numbers (of real numbers) with supporting intervals of $[l_1, l_2]$ and $[k_1, k_2]$. Here, the k_1, l_1 and k_2, l_2 signifies the lower limits and upper limits (endpoints), respectively. k_2-k_1 and l_2-l_1 are the interval widths determined for intervals K and L, respectively. Addition, subtraction, multiplication, division, minimization, and maximising are all mathematical operations that may be applied to interval numbers [22].

$$K + L = [k_1 + l_1, k_2 + l_2] \tag{1}$$

$$K - L = [k_1 - l_2, k_2 - l_1] \tag{2}$$

$$K \times L = [min.(k_1 \times l_1, k_1 \times l_2, k_2 \times l_1, k_2 \times l_2), max.(k_1 \times l_1, k_1 \times l_2, k_2 \times l_1, k_2 \times l_2)] \tag{3}$$

$$\frac{K}{L} = K \times L^{-1} \tag{4}$$

where $L^{-1} = [1/l_2, 1/l_1]$ with $0 \notin [l_1, l_2]$.

The distance between K and L is defined as

$$d(K, L) = max[|k_1 - l_1|, |k_2 - l_2|] \tag{5}$$

Complex uncertainty can be obtained by representing real numbers in complex domain. The PF study utilizes the above-mentioned fundamental operations to calculate the link between uncertain variables in terms of complex interval numbers. In this research, IA is used to deal with the uncertainties in the N/w data. Therefore, reactance, resistance, bus voltage and N/w power loss are taken as interval numbers instead of a fixed value. Rather than the fixed variation discussed in section 3.2, the N/w load at a bus is assumed to fluctuate over a specified range based on a Gaussian distribution. When the load demand is changing over the interval, the number of PF computations required are lesser than the total number of repeated PF solutions.

3. MATHEMATICAL MODEL

3.1. Line variation model

Fig. 1 is a one-line diagram of a branch connecting bus i-1 and bus i.
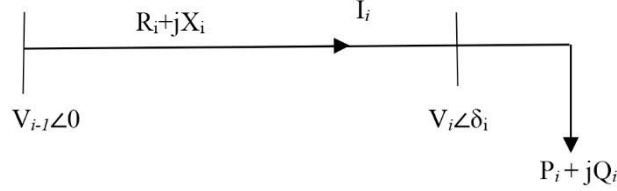
Fig. 1 Single branch equivalent

From Fig. 1,

$$P_i + jQ_i = V_i \angle \delta_i . I_i^*$$ (6)

where, V_i stands for receiving-end rms bus voltage and δ_i is voltage angle at bus i. The reactive and real power load fed through the ith bus are represented by Q_i and P_i, respectively. Every bus, including the source bus, has an initial voltage of [1.0,1.0] +j [0.0,0.0] p.u. Since, both power and voltage are complex interval variables, the subsequent current at bus i (I_i), as described in (7), is also a complex interval quantity that can be evaluated using the division operation (4).

$$I_i = \frac{\left[P_{i_{lo}}, P_{i_{up}}\right] - j\left[Q_{i_{lo}}, Q_{i_{up}}\right]}{V_i \angle - \delta_i}$$ (7)

where $P_{i_{lo}}$, $Q_{i_{lo}}$ and $P_{i_{up}}$, $Q_{i_{up}}$, respectively, are lower and the higher limits for the real and reactive power load at the ith bus. The N/w real and reactive loss in a branch is

$$P_{loss}(i-1,i) = \frac{(P_i^2 + Q_i^2)}{|V_i|^2} . R_i$$ (8)

$$Q_{loss}(i-1,i) = \frac{(P_i^2 + Q_i^2)}{|V_i|^2} . X_i$$ (9)

The branch reactance and resistance, respectively, are X_i and R_i. At a constant proportion, the line parameter's uncertainty can be introduced as

$$X_{ilo} = (1 - \%(X)). X_i$$ (10)

$$X_{iup} = (1 + \%(X)). X_i$$ (11)

$$R_{ilo} = (1 - \%(R)). R_i$$ (12)

$$R_{iup} = (1 + \%(R)). R_i$$ (13)

where R_{ilo}, X_{ilo} and R_{iup}, X_{iup} are the lower and the upper constraints on the N/w resistance and reactance, respectively.

3.2. Variation in Load Model

In the RDN, the majority of the loads are frequency and voltage-dependent [23]. For analyzing static load, only variation in voltage is considered as deviation in frequency is not significant [24]. The load model generally chosen is complex power type, but in reality, the load is a combination of numerous load models. Therefore, this study aims at evaluating the impact of realistic load models viz. industrial, residential and commercial loads in the distribution N/w that is particularly important for DNOs in various planning scenarios. The considered load models can be expressed mathematically as [25].

$$P_i = P_{ino} \cdot \left(\frac{|V_i|}{|V_{ino}|} \right)^{x1} \tag{14}$$

$$Q_i = Q_{ino} \cdot \left(\frac{|V_i|}{|V_{ino}|} \right)^{x2} \tag{15}$$

where x1 and x2 are the load exponents. Q_{ino} is the nominal reactive load, P_{ino} is the rated real load and V_{ino} is the rated bus voltage at the ith bus, respectively. In the present study, the real and reactive exponents taken for constant power load (CPL), industrial load (IL), residential load (RL) and commercial load (CML) model are 0 & 0, 0.18 & 6.00, 0.92 & 4.04 and 1.51 & 3.40, respectively [25]. As practically any type of load might present in the N/w, therefore, composite load (CL) model is considered for the analysis with 40% of CPL, 30% of IL, 20% of RL and 10% of CML [25].

The Gaussian distribution function is utilized to predict the change in N/w power load demand. The Gaussian distribution is a symmetric mean-value distribution with a bell-shape and mentioned as (16)

$$f(yi) = \frac{1}{\sqrt{2\pi\sigma^2}} e^{-\frac{1}{2} \frac{(yi-\mu)^2}{\sigma^2}} \tag{16}$$

Where random variables σ^2 and μ are distribution parameters that represents variance and mean (expected) value of the base loads, respectively. The variance represents how much the random variable is expected to deviate from its mean value (in a certain percentage). The normalised value of the reactive or real power load at bus i of the considered network is given by yi, which can be given as in [17].

$$yi = \frac{P_i}{P_{ino}} \text{ and } yi = \frac{Q_i}{Q_{ino}} \tag{17}$$

where, (14) and (15) defines P_i and Q_i, respectively.

$\alpha_{ql}(k)$ and $\alpha_{pl}(k)$ are the degree of belongingness for reactive and real power load, where k indicates a number of degree of belongingness. From the load curve illustrated in Fig. 2 the mean value of the normalized real and reactive power load is unity for the degree of belongingness 1.0. The degree of belongingness can have any value between $\alpha_{pl_{max}} / N$ and $\alpha_{pl_{max}}$ where, the number of points of linearization of the Gaussian curve is denoted by N and $\alpha_{pl_{max}}$ is the maximum degree of belongingness. The Gaussian distribution curve for a real power load is depicted in Fig. 2 [17].
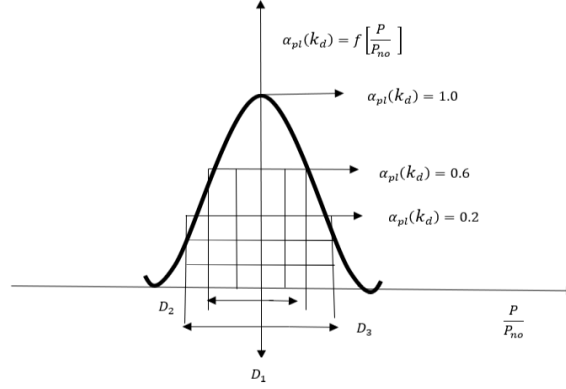
Fig. 2 Gaussian distribution of load

Equation (16) can be written as

$$\alpha_{pl}(k_d) = f\left[\frac{P_i}{P_{ino}}\right] = \frac{1}{\sqrt{2\pi\sigma^2}}e^{\left[\frac{P_i}{P_{ino}}-\mu\right]^2 \Big/ 2\sigma^2} \tag{18}$$

From equation (18), we get $\sigma = 0.399$ for $\mu = 1.0$ and $\alpha_{pl}(k_d) = 1.0$.
For these values, equation (18) can be written as

$$\frac{P_i}{P_{ino}} - 1 = \pm\sqrt{\frac{-\ln(\alpha_{pl}(k_d))}{\pi}} \quad \text{for } \frac{P_i}{P_{ino}} \neq 1 \tag{19}$$

Similarly, for reactive load

$$\frac{Q_i}{Q_{ino}} - 1 = \pm\sqrt{\frac{-\ln(\alpha_{ql}(k_d))}{\pi}} \quad \text{for } \frac{Q_i}{Q_{ino}} \neq 1 \tag{20}$$

Right Hand Side of equation (19) and (20) can be specified as

$$\sqrt{\frac{-\ln(\alpha_{pl}(k_d))}{\pi}} = \alpha_K = \sqrt{\frac{-\ln(\alpha_{ql}(k_d))}{\pi}} \tag{21}$$

Thus, (19) can be rewritten as

$$\frac{P_i}{P_{ino}} = 1 \pm \alpha_{K_d} \tag{22}$$

$$P_i = P_{ino}(1 \pm \alpha_{K_d}) \tag{23}$$

where $\pm$ sign gives a lower and upper constraints of the N/w load at bus i.

$$P_{i_{lo}} = P_{ino}(1 - \alpha_{k_d}) \tag{24}$$
$$P_{i_{up}} = P_{ino}(1 + \alpha_{k_d}) \tag{25}$$
$$Q_{i_{lo}} = Q_{ino}(1 - \alpha_{k_d}) \tag{26}$$
$$Q_{i_{up}} = Q_{ino}(1 + \alpha_{k_d}) \text{ where } k_d = 1, 2..N \tag{27}$$

Linearization at different k_d values in equations (24)-(27) results in k_d discrete load intervals in closed form. For the analysis purpose, the linearization is carried out at three

different points which results in three distinct load intervals (D-regions) as shown in Fig. 2 and given below

$$D_1 \rightarrow \{P_{ino}, P_{ino}\} \quad \text{point interval for } k_d=1 \tag{28}$$

$$D_2 \rightarrow \{P_{ino}[1 - \alpha_2], P_{ino}[1 + \alpha_2]\} \quad \text{for } k_d=2 \tag{29}$$

$$D_3 \rightarrow \{P_{ino}[1 - \alpha_3], P_{ino}[1 + \alpha_3]\} \quad \text{for } k_d=3 \tag{30}$$

Equations (28)-(30) shows that the D_1, D_2 and D_3 are in bound form. Therefore, an IA operation has been implemented to introduce these variations in the power flow.

3.3. DG Modelling

The generator bus has been characterised as a continuous negative PQ load for the small size DG resources, implying that they run in constant power mode. According to the IEEE 1547 Standard [26] the DGs are not meant for regulating the voltage at the buses as they may conflict with the utilities' existing distribution voltage regulating schemes [27]. The total N/w load gets reduced by the power generated by the connected DG. The solar PV-DG injects real power at unity power factor. The resultant load at bus i at which solar-PV DG has been placed will be

$$P_{rei} = P_i - P_{solar\ PV-DGi} \tag{31}$$

where, $P_{solar\ PV-DGi}$ represents real power injected by the solar PV-DG at bus i.

4. PSO ALGORITHM

PSO is a stochastic technique in which each particle in a search space alters its state. In a d-dimensional hyperspace, the updated particle velocity and position are expressed as:

$$v_{pd}^{n+1} = w_p v_{pd}^n + c_1 rand_1(pbest_{pd} - S_{pd}^n) + c_2 rand_2(gbest_{pd} - S_{pd}^n) \tag{32}$$

$$S_{pd}^{n+1} = S_{pd}^n + v_{pd}^{n+1} \tag{33}$$

where, S_{pd}^n and v_{pd}^n shows the particle's current position and velocity at n^{th} iteration, respectively. $p = 1,2,...N_s$ where N_s represents the swarm size. The acceleration coefficients for the IInd and Ist particles are c_2 and c_1, respectively. Random numbers in the interval [0,1] are $rand_1(.)$ and $rand_2(.)$. $pbest_{pd}$ and $gbest_{pd}$ are particle personal best and the global best position, respectively. The particle p's inertia weight (w_p) is given as

$$w_p = w_{pmax} - \frac{(w_{pmax} - w_{pmin})}{n_{max}}.n \tag{34}$$

where, w_{pmin} and w_{pmax} are the minimum and the maximum inertia weight value, respectively. n_{max} and n are the maximum and current iteration number, respectively.

5. DEVELOPMENT OF NOVEL VSI AND OPTIMAL ALLOCATION OF SOLAR PV-DG

A novel VSI is proposed to site DG optimally and is derived by substituting the value of I_i from (6) in V_i, we get

$$V_i \angle \delta_i = V_{i-1} \angle 0 - \left[(R_i + jX_i).\left(\frac{P_i - jQ_i}{V_i \angle -\delta_i} \right) \right] \tag{35}$$

By multiplying (35) with $V_i \angle - \delta_i$ on both sides, we obtain

$$V_i^2 = V_{i-1}V_i \angle - \delta_i - (R_i + jX_i)(P_i - jQ_i) \tag{36}$$

$$V_i^2 + [P_iR_i + Q_iX_i + j(P_iX_i - Q_iR_i)] = V_{i-1}V_i \cos \delta_i - jV_{i-1}V_i \sin \delta_i \tag{37}$$

On segregation of real and imaginary part of (37), we obtain

$$V_i^2 + P_iR_i + Q_iX_i = V_{i-1}V_i \cos \delta_i \tag{38}$$

$$P_iX_i - Q_iR_i = -V_{i-1}V_i \sin \delta_i \tag{39}$$

Substituting X_i from (39) in (38), we obtain

$$V_i^2 + P_iR_i + Q_i.(\frac{Q_iR_i - V_{i-1}V_i \sin \delta_i}{P_i}) = V_{i-1}V_i \cos \delta_i \tag{40}$$

$$V_i^2 - \frac{Q_iV_{i-1}V_i \sin \delta_i}{P_i} - V_{i-1}V_i \cos \delta_i + P_iR_i + \frac{R_iQ_i^2}{P_i} = 0 \tag{41}$$

$$V_i^2 + (-\frac{Q_iV_{i-1} \sin \delta_i - P_iV_{i-1} \cos \delta_i}{P_i})V_i + R(P_i + \frac{RQ_i^2}{P_i}) = 0 \tag{42}$$

For bus voltages to be stable, (42) must have real roots, i.e. discriminant > 0 that resulted in the proposed VSI for the given branch and can be articulated as in (44)

$$(\frac{-Q_iV_{i-1} \sin \delta_i - P_2V_{i-1} \cos \delta_i}{P_i})^2 - 4R_i(P_i + \frac{R_iQ_i^2}{P_i}) \leq 0 \tag{43}$$

$$\frac{4R_i.P_i^2}{(Q_iV_{i-1} \sin \delta_i + P_iV_{i-1} \cos \delta_i)^2} \cdot \left(P_i + \frac{Q_i^2}{P_i}\right) \leq 1 \tag{44}$$

The bus voltage determined from the PF solution is utilised to calculate VSI for each branch that lies in [0,1] range. Any value of proposed VSI nearing 0 shows stable operation, in contrary, VSI value approaching 1 indicates that the bus is gradually leading towards instability.

The constraints taken for the analysis:
a) Power balance:

$$P_G = P_D + P_{loss} \tag{45}$$

$$Q_G = Q_D + Q_{loss} \tag{46}$$

where Q_G and P_G shows the reactive and real power generated. Q_D and P_D stands for reactive and real load demand on the network.
b) Voltage constraint:

$$0.95 \, p.u \leq V_i \leq 1.05 \, p.u \tag{47}$$

c) Current constraint:

$$I_{branch} \leq I_{thermal} \tag{48}$$

where, I_{branch} and $I_{thermal}$ shows the branch current and its thermal limit, respectively.
d) DG power generation constraint:

$$0 \leq P_{solar \, PV-DGi} \leq \sum P_{Load} \tag{49}$$

where $\sum P_{Load}$ is the total real power load in the network.
e) Substation capacity:

$$0 \leq P_g^i \leq P_{g(max)} \quad i \in \text{slack} \tag{50}$$

$$0 \leq Q_g^i \leq Q_{g(max)} \tag{51}$$

where $Q_{g(max)}$ and $P_{g(max)}$ represents the maximum value of reactive and real power generation, respectively. Q_g^i and P_g^i shows the reactive and real generated power at the slack bus, respectively.

The pseudo-code for the optimal integration of solar PV-DG for the deterministic case in the RDN is mentioned below:

Step I: Run the PF program to calculate the bus magnitude and its phase angle, branch current, N/w power losses using direct PF method [28] of RDN for the base case. The following iterative formula is used to determine the solution

$$[V_i^n] = [V_i^0] + [BCBV][BIBC][I_i^{n-1}] \tag{52}$$

where, BCBV stands for Branch Current-to-Bus Voltage and BIBC stands for Bus Incidence-to-Branch current matrix. The initial voltage (V_i^0) is 1.0 +j 0 p.u. I_i^{n-1} is the branch current at n-1 iteration and V_i^n is the bus voltage at nth iteration at bus i.

Step II: Determine the cost of annual energy loss [29] using

$$Annual\ cost\ of\ energy\ losses\ = (\sum_{i=2}^{NB} P_{Loss}\ (i-1,i)\ T.E\ )\ \$ \tag{53}$$

where NB is the number of buses, T is the annual time duration (8760 hrs) and E is cost of energy (0.06 \$/kWh).

Step III: Evaluate VSI using (44). Select bus i as the most sensitive bus to place DG if a branch between bus i-1 and i has the greatest VSI value.

Step IV: Set PSO parameters (swarm size, inertia weights, acceleration coefficients) for minimizing real power loss (RPL).

Step V: Set iteration counter (n) to 0.

Step VI: With random velocities and placements on the dimension as pbest, the values of solar PV-DG size are created (between 0 and $\sum$ system loads (continuous)).

Step VII: After installing DG at the location as obtained in step III, repeat the PF algorithm for each particle. Calculate RPL for the randomly initialised particles if all constraints are within limits. Otherwise, discard the infeasible solution.

Step VIII: The solar PV-DG size giving minimum RPL value is opted as gbest and its corresponding position is considered as the particle best position.

Step IX: The particles' velocity, position and the weight are updated utilizing (32), (33) and (34), respectively.

Step X: If maximum iterations (n_{max}) are reached, jump to Step XI. Otherwise, the counter is incremented and steps IV through X are repeated. If the newly obtained particle position is superior to the prior pbest and gbest, new pbest and gbest will be generated.

Step XI: The best location denotes optimal solar PV-DG sizes, while the corresponding number denotes the lowest total RPL.

Step XII: Determine annual power loss savings after calculating the cost of energy losses in the presence of DG using (53).

6. INTERVAL-BASED B/F PF SOLUTION METHODOLOGY

The following steps are used to determine the value of the bus voltage and N/w losses:

Step I: Read N/w data.

Step II: Determine the degree of belongingness $\alpha_{pl}(k_d)$ and $\alpha_{ql}(k_d)$ for N intervals.

Step III: Complex interval numbers V_i^n and V_i^0 can be written as $V_i^n = A_1 + jA_2$ and $V_i^0 = B_1 + jB_2$ where A_1, A_2, B_1 and B_2 are all interval numbers. The voltage start for all buses is [1.0,1.0] +j [0.0,0.0] p.u. At first, N/w losses are set to zero. The iteration count and slack bus angle are initialized to zero.

Step IV: Calculate the equivalent real power load at the bus using (31) after optimal siting and sizing of solar PV-DG as explained in step III and step XI of section 5, respectively.

Step V: The closed bounded interval of line and load data is determined from (10) through (13) and (24) through (27), respectively for the various degree of belongingness.

Step VI: For the complex nature of the load, update the bounded interval of real and reactive power load with the use of (14) and (15).

Step VII: Form BIBC, BCBV and distribution PF matrices.

Step VIII: Determine the currents and voltages at each bus using (7) and (52) using subtraction, addition, division and multiplication operation of the complex interval numbers as described in section 2.

Step IX: The voltage difference between two successive iteration can be given as

$$V_i^n - V_i^0 = \max[d(A_1, B_1), d(A_2, B_2)] \tag{54}$$

where $d(A_1, B_1)$ and $d(A_2, B_2)$ is calculated using (5). If $\max[d(A_1, B_1), d(A_2, B_2)] < 10^{-4}$ at all the buses then jump to step X, else jump to step V.

Step X: Use (8) and (9) to calculate N/w power losses.

Step XI: Print the results for specific value of $\alpha_{pl}(k_d)$ and $\alpha_{ql}(k_d)$.

Step XII: If k_d=N terminate the program otherwise increment k and go to step II.

7. RESULTS AND DISCUSSION

To demonstrate the performance of the IA-based PF technique in the presence of various realistic loads and solar PV-DG, IEEE distribution test networks of varying complexity and size are simulated to show its robustness. The complete N/w data for 33- and 69-bus N/w has come from [30] and [31], respectively. For both networks under consideration, the base kV and MVA are 12.66 and 100, respectively. The bus feeders of IEEE N/w were tested on MATLAB. A voltage error tolerance of 0.0001 p.u is considered for all the test cases acknowledged in this work. The piecewise segmentation of annual load profile in light, nominal and heavy load level is assumed 50%, 100% and 160% of the rated N/w load [32] with an annual hourly duration of 1000, 6760, and 1000 hours [11], respectively. To confirm the efficacy of the suggested methodology, the simulated network performance is compared to previously published findings for deterministic parameters for the same base voltage and the load model.

In Table 1, the power flow results at various realistic loads for 33-bus RDN are compared to the published literature. The N/w real and reactive power losses are 5.5% and 5.9% of their respective load for CPL model, whereas, for CL model the real and reactive

losses reduces to 4.7% and 5.04%, respectively. The convergence is also faster when compared to that of [25].

Table 1 Power flow result at various load models for 33-bus RDN

	Proposed method					[25]				
Type of load	CPL	IL	RL	CML	CL	CPL	IL	RL	CML	CL
Total RPL (kW)	202.66	161.28	158.54	153.57	174.21	202.68	161.69	159.33	154.93	174.19
Total reactive power loss (kVAr)	135.13	107.20	105.31	101.94	115.89	135.23	107.56	105.92	102.94	115.97
Number of iterations	4	2	2	2	2	3	4	4	4	3

Assuming constant annual load with only one type of load model is a misnomer because the N/w load profile is highly affected by various type of load model and time variations, hence light load, nominal load and heavy load levels are considered. The V_{min} and network power losses attained for IEEE 69-bus N/w at different load levels for CPL and CL model are mentioned in Table 2. For 69-bus N/w, the power losses and the convergence characteristics obtained for deterministic case are compared at a nominal load in Table 3 to exemplify the capability of the proposed method.

From Table 2, it is inferred that the reduction in load has a positive effect on N/w bus voltage profile, while increment in load aggravates it, in both cases. For 69-bus RDN, the bus voltage profile attained with CL and CPL model is given in Fig. 3. The results demonstrate that the effect of CL model on N/w performance is over-represented as compared to CPL model. As the N/w power loss reduction varies unproportionate to the network load, thus, it is better to provide generalized equations for the N/w power losses using a curve fitting. The generalized power loss equations for CPL and CL model are as follows:

For CPL,
$$P_{loss}(kW) = 332.11\lambda^2 - 151.68\lambda + 44.37 \tag{55}$$
$$Q_{loss}(kVAr) = 147.98\lambda^2 - 64.88\lambda + 18.98 \tag{56}$$

For CL,
$$P_{loss}(kW) = 149.22\lambda^2 + 20.51\lambda - 3.71 \tag{57}$$
$$Q_{loss}(kVAr) = 69.28\lambda^2 + 9.24\lambda - 1.73 \tag{58}$$

where, λ represents load level. The general expressions from (55) to (58) are useful for DNOs in future power generation planning.

Table 2 Results of 69-bus N/w at various load levels with no solar PV-DG

	CPL			CL		
Load level	Light	Nominal	Heavy	Light	Nominal	Heavy
V_{min} (p.u.)	0.9567	0.9092	0.8446	0.9597	0.9211	0.8757
RPL (kW)	51.56	224.80	651.88	43.85	166.02	411.11
Reactive power loss (kVAr)	23.54	102.09	294.02	20.21	76.79	190.41

Table 3 Comparative analysis of CL model at nominal load and without DG for 69-bus RDN

	Proposed method	[25]
RPL (kW)	166.02	189.3761
Reactive power loss (kVAr)	76.79	86.8497
Number of iterations	2	3
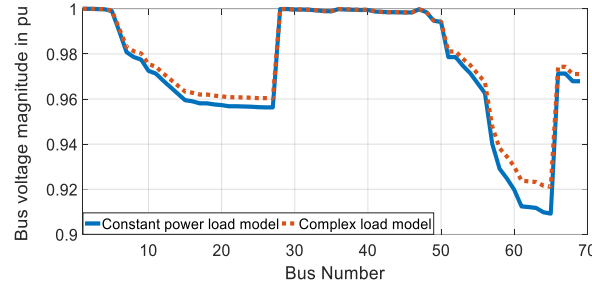
Fig. 3 Voltage profile of 69-bus RDN with CPL and CL model

Validation of novel VSI

To authenticate the index, the N/w load (P and Q both) is subjected to the random variation between 0 and 160% of the total base load. For 69-bus N/w, branch 60 with 0.0286 value is determined to have the largest VSI value. As a result, the bus 61 is regarded the most vulnerable bus beyond critical loading and is investigated as the load increases. Fig. 4 displays the VSI variation at the critical bus at various loading conditions. As VSI displays a linear variation to N/w load increment, it can be utilized for the accurate prediction of the voltage stability in RDN as also concluded in [32].
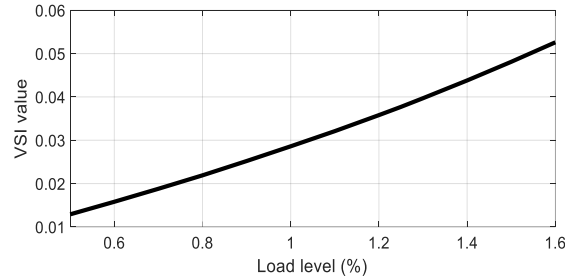
Fig. 4 Variation in the value of VSI at various load levels in 69-bus RDN

7.1. Analysis of N/w performance with optimal integration of solar PV-DG

The proposed methodology has been employed on 69-bus RDN for the optimal integration of Solar PV-DG having deterministic parameters. The n_{max} and swarm size is 130 and 20, respectively. To achieve fast convergence of the optimization technique, the control variables c_1 and c_2 value in (32) and w_{pmax} and w_{pmin} in (34) are chosen as 2, 2,

0.9 and 0.4, respectively [33]. The value of VSI for each branch of 69-bus RDN is shown in Fig. 5. Bus 61 is found out to have the maximum VSI value and is chosen as the best DG placement location at nominal load level.
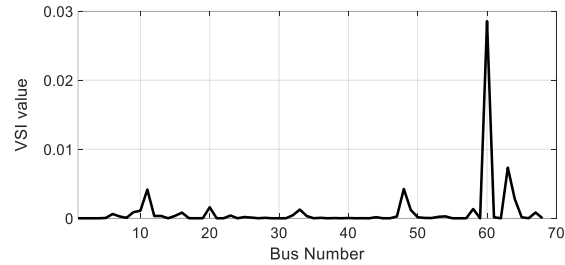
Fig. 5 VSI at each branch in 69-bus RDN

The optimal size and site of solar PV-DG is determined at various loading scenarios using the proposed method. The DG size follows a linear relationship with N/w load increment for the 69-bus network, as exemplified in Fig. 6. The N/w performance in terms of V_{min}, power losses, RPL reduction and cost of annual energy losses attained at nominal load level after integrating solar PV-DG for CPL and CL model is illustrated in Table 4.

Table 4 Results for solar PV-DG at nominal load level

	Base case	CPL	CL
Optimal DG location @ Solar PV-DG size in kW	-	61 @ 1888	61 @1888
V_{min} in pu @ bus (% voltage improvement)	0.9092 @ 65	0.9684 @ 27	0.9700 @ 27
		(6.5 %)	(6.7 %)
RPL (kW)	224.80	83.17	70.40
RPL reduction (kW)	-	141.63	154.40
(in %)		(63.00%)	(68.68)
Reactive power loss (kVAr)	102.09	40.51	34.88
(in %)		(60.31%)	(65.83%)
Annual cost of energy loss ($)	91178.88	33733.75	28554.24
AELS ($)	-	57445.13	62624.64
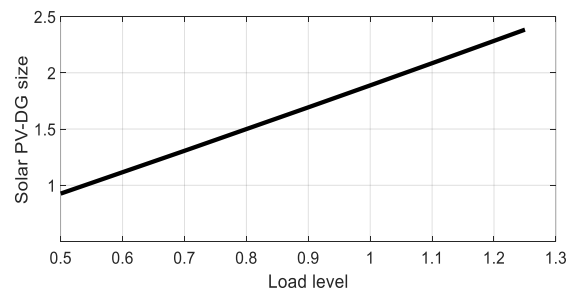
Fig. 6 Optimal Solar PV-DG size at various load levels in 69-bus network

7.1.1. Impact of solar PV-DG on N/w power loss

The integration of solar PV-DG has a considerable effect on N/w losses. To validate, the general mathematical expressions of P_{loss} and Q_{loss} for any load level in the 69-bus N/w are derived utilizing curve fitting approach as depicted below

For CPL model,
$$P_{loss}(kW) = 92.40\lambda^2 - 12.87\lambda + 3.64 \tag{59}$$
$$Q_{loss}(kVAr) = 44.68\lambda^2 - 5.8\lambda + 1.64 \tag{60}$$

For CL model,
$$P_{loss}(kW) = 55.15\lambda^2 + 20.76\lambda - 5.51 \tag{61}$$
$$Q_{loss}(kVAr) = 28.21\lambda^2 + 9.09\lambda - 2.42 \tag{62}$$

After comparing N/w power losses without DG [(55) - (58)] and with solar PV-DG [(59) – (62)], we can conclude that the integration of renewable DG minimises the N/w losses at all load levels for all types of load models.

The relationship between the variation in RPL with solar PV-DG size for 69-bus RDN considering CL model is illustrated in Fig. 7, which seems to follow a parabolic curve. The curve shows the RPL value decreases with the increase in the size of solar PV-DG as presented in the left portion of the curve. The optimum DG size will be attained at the lowest point of the curve when RPL reached to its minimum value after which the RPL losses increase as DG size increases (right part of the curve) due to extra current flow from the DG to the adjacent bus. The RPL in 69-bus RDN without integrating solar PV-DG was found to be 224.80 kW and 166.02 kW for CPL and CL model, respectively. After optimal integration of solar PV-DG, the RPL for CPL and CL model in IEEE 69-bus N/w mitigates to 83.17 kW and 70.40 kW with a decrease of 63.00% and 68.68% percent, respectively, with respect to the base case (From Table 2). The real power demand released is 141.63 kW for the CPL model and 154.40 kW for the CL model after installing SPV-DG, respectively. The RPL magnitude at each branch with and without solar PV-DG is demonstrated in Fig. 8 for 69-bus N/w with CPL model at nominal load. The results validate that the N/w loss minimizes after integration of solar PV-DG.
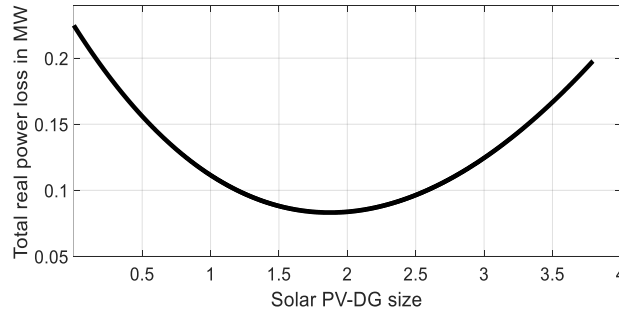
Fig. 7 Relationship between RPL and solar PV-DG size at optimal DG bus in 69-bus N/w
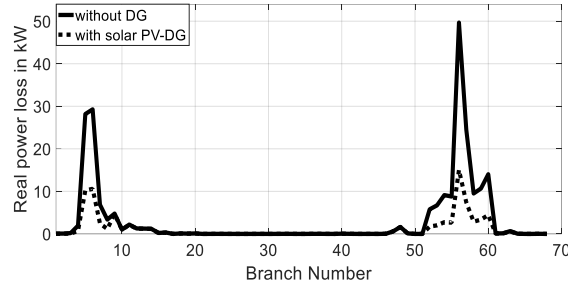
Fig. 8 Network RPL with and without renewable DG at nominal load in 69-bus RDN

7.1.2. Impact of solar PV-DG on bus voltage profile

The V_{min} for 69-bus N/w has been updated from 0.9092 pu at bus 65 to 0.9684 pu and 0.9700 pu at bus 27 for CPL and CL models, respectively, resulting in 6.5 % and 6.7 % increase in bus voltage magnitude (From Table 4). It has been found out that for both the load model the N/w voltage profile is enhanced after solar PV-DG installation satisfying the constraints.
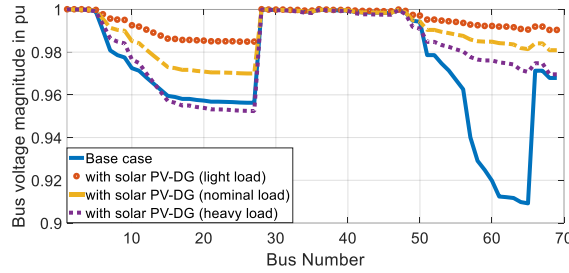
Fig. 9 Impact of N/w load variation on voltage profile in 69-bus N/w for CL model

The effect of different load levels on bus voltage profile considering realistic loads is analysed in Fig. 9 and found out to have a remarkable enhancement in voltage profile for 69-bus N/w at all the considered load levels after installing solar PV-DG. Fig. 9 also shows that all the bus voltages attained from the proposed method are within allowable voltage limits and hence validates the method consistency. Thus, the obtained integrated solution is very beneficial for DNOs.

7.1.3. Impact of solar PV-DG on AELS

The cost of energy loss in 69-bus RDN before integrating solar PV-DG was $91178.88 which is reduced to $33733.75 and $28554.24 with solar PV-DG resulting in AELS of $57445.13 and $62624.64 for CPL and CL model, respectively, at nominal load level with respect to the base case as mention in Table 4. The AELS for CPL and CL model attained considering all the load levels are $85257.73 and $93577.34, respectively compared to base case.

7.1.4. Comparative analysis

To authenticate the efficacy of the method, the test results attained after the penetration of solar PV-DG are compared to other available meta-heuristic methods like WOA [34], GWO [35], PSO [36], SGA [36], CSA [36] and BB-BC [37] and mentioned in Table 5 for the 69-bus N/w. Due to the variable nature of RPL reduction and DG size, it becomes obligatory to compare it on a common platform which is carried out by calculating the ratio of RPL reduction to size of DG. The penetration of solar PV-DG in the N/w yields a ratio of 0.075 superior or comparable to already published literature. The higher value of the ratio compared to the already published results signifies the robustness of the proposed approach used for the optimal integration of DG. To demonstrate its rapid convergence, the computational time required for solar PV allocation at a nominal load for the 69-bus N/w is calculated and compared to the existing literature [38] and [12] (Table 6).

Table 5 Comparative analysis of solar PV-DG integration techniques for 69-bus N/w

DG allocation method	Size of DG/ power factor	Optimum Location	RPL (kW)	% RPL reduction	Ratio of RPL reduction to solar PV-DG size
Proposed approach	1888/1	61	83.17	63.00	0.075
WOA [34]	1872.82/1	61	83.23	63.01	0.075
GWO [35]	1928.67/1	61	83.24	62.98	0.073
PSO [36]	2000/1	61	83.80	62.75	0.070
CSA [36]	2000/1	61	83.80	62.74	0.070
SGA [36]	2300/1	61	89.40	60.30	0.058
BB-BC [37]	1872.5/1	61	83.22	63.00	NR

NR: Not Reported

Table 6 Execution time for solar allocation at nominal load in 69-bus N/w

	Proposed method	Analytical method [38]	GA [12]
CPU time (sec)	0.20	0.70	0.85

7.2. Analysis of N/w uncertainties (line and load) with optimal integration of solar PV-DG

For the comparative analysis, the load and line uncertainties for the CPL model are set to 5% and 1%, respectively as described in [19] for IEEE 33-bus RDN. The interval width for line and load uncertainty at V_{min} is tabulated and compared with FAA [19] in Table 7. The results clearly illustrate that the interval width determined from the proposed probabilistic-possibilistic approach is narrower. As a result, the solution is less conservative and superior to the probabilistic technique alone. It can be concluded that increasing N/w load uncertainty creates a bigger voltage drop than increasing N/w line uncertainty.

Table 7 Interval width of V_{min} for CPL model in 33-bus N/w

Output variable	Type of uncertainty	Interval width (p.u)		Interval width reduction in %
		Probabilistic-possibilistic approach	FAA [19]	
V_{min} (p.u)	Line	0.0019	0.0021	9.5
	Load	0.0094	0.0142	33.8

In this case, the analysis of uncertainties in input parameter is presented with solar PV-DG for 69-bus N/w. The fixed variation of $\pm3\%$ in N/w line data has been considered. The solar PV-DG is positioned at bus 61 with DG size of 1888 kW as determined in case 1 from the proposed method.

The simulated results for V_{min}, total real and reactive N/w losses in solar PV-DG integrated IEEE 69-bus N/w for the deterministic case and when uncertainties occur in N/w line and load parameter at various degree of belongingness at different load models are tabulated in Table 8. At $\alpha = 1$, the interval widths for CPL, IL, RL, CML, and CL are 0.002 pu, 0.0017 pu, 0.0017 pu, 0.0016 pu, and 0.0018 pu, respectively, based on the upper and lower bounds of the V_{min}. For all practical load models, the interval of voltage magnitude at bus 65 is narrower than that obtained from the CPL load model. As a result, the CL model, as opposed to the CPL model, produces more realistic results. Fig. 10 shows the effect of adding uncertainties on the voltage profile of 69-bus N/w for the CL model and three degrees of belongingness ($\alpha = 0.2, 0.6, 1$). As expected, with deterministic input values, the voltage magnitude at every bus fall within the range of potential N/w states obtained by varying input parameters.

Table 8 Results for IEEE 69-bus N/w with load and line uncertainty and DG penetration at nominal load

Degree of belongingness		Deterministic result	$\alpha_{pl}, \alpha_{ql} = 1$		$\alpha_{pl}, \alpha_{ql} = 0.6$		$\alpha_{pl}, \alpha_{ql} = 0.2$	
Load model		Deterministic result	Lower	Upper	Lower	Upper	Lower	Upper
CPL	V_{min}	0.9684	0.9674	0.9694	0.9535	0.9820	0.9425	0.9915
	P_{loss}	83.1722	80.5589	85.7935	28.1596	172.5547	6.3011	262.4480
	Q_{loss}	40.5177	39.2487	41.7903	13.7375	83.9240	3.0769	127.4850
IL	V_{min}	0.9709	0.9700	0.9717	0.9586	0.9828	0.9499	0.9916
	P_{loss}	60.4966	59.1220	61.8500	23.3002	110.3419	6.0157	153.6309
	Q_{loss}	30.499	29.7787	31.2103	11.5943	56.3890	2.9513	79.266
RL	V_{min}	0.9710	0.9702	0.9719	0.9590	0.9829	0.9507	0.9916
	P_{loss}	65.6427	64.0243	67.2424	24.5247	122.8959	6.0953	173.7163
	Q_{loss}	32.7774	31.9483	33.5982	12.1344	61.9703	2.9863	88.2260
CML	V_{min}	0.9714	0.9706	0.9722	0.9599	0.9830	0.9519	0.9916
	P_{loss}	67.1456	65.4526	68.8209	24.8706	126.6893	6.1169	179.9339
	Q_{loss}	33.4364	32.5746	34.2904	12.2859	63.6350	2.9957	90.556
CL	V_{min}	0.9700	0.9691	0.9709	0.9569	0.9825	0.9476	0.9916
	P_{loss}	70.40	68.5249	72.2729	25.5387	136.0021	6.0119	196.6515
	Q_{loss}	34.88	33.9405	35.8256	12.5824	67.7841	2.9496	98.4141
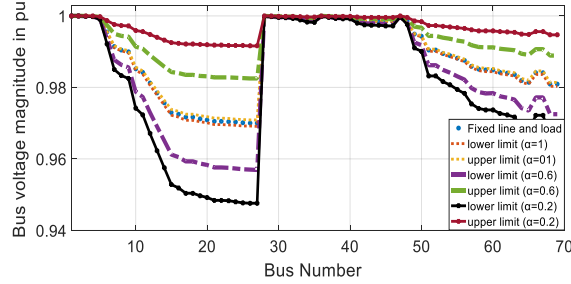
Fig. 10 Voltage profile with solar PV-DG with fixed and varying line and load parameter at various degree of belongingness considering CL model and nominal load

Fig. 11 shows the variation of total reactive and real power losses at different degree of belongingness without and with solar PV-DG for the CL model in IEEE 69-bus N/w. It was obvious that when solar PV-DG was integrated into an IEEE 69-bus N/w, power losses were dramatically decreased. As can be seen in Fig. 11, the interval between power losses reduces as the degree of belongingness increases.
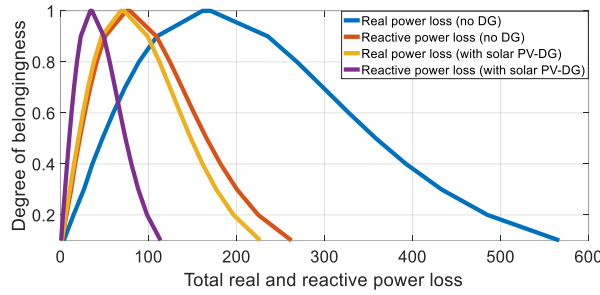
Fig. 11 Variation of total N/w losses at different degree of belongingness with CL model at nominal load level

The generalized equations for determining lower and upper real and reactive losses in 69-bus RDN considering the CL model with line and load uncertainty at α=0.6 using curve fitting technique are given as

$$P_{loss_{lo}}(kW) = 22.02\lambda^2 + 5.15\lambda - 1.3 \qquad (63)$$
$$Q_{loss_{lo}}(kVAr) = 11.05\lambda^2 + 2.12\lambda - 0.577 \qquad (64)$$
$$P_{loss_{up}}(kW) = 97.50\lambda^2 + 52.05\lambda - 13.55 \qquad (65)$$
$$Q_{loss_{up}}(kVAr) = 50.88\lambda^2 + 22.86\lambda - 5.96 \qquad (66)$$

The coefficient of variation (CV) in RPL decreases with the penetration of solar PV-DG with CL model for 69-bus N/w, and is greatest for the base case, as tabulated in Table 9. This implies that the integration of DG decreases the power loss variation in the feeders of the distribution N/w around its mean value and thereby provide better security against overheating of feeders and instability. It is found that the CL model provide better results consistently as specified by their better voltage profile, lowest power losses and minimum

CV. The minimum, maximum, mean, standard deviation (Std) and CV of power loss lies within their lower and upper limits for all values of α but has been illustrated for α =1 only, in Table 9. It has been observed that higher the DG penetration, higher will be the CV value due to its higher degree of uncertainty.

Table 9 Statistical analysis for RPL without and with DG in IEEE 69-bus N/w with CPL and CL model and uncertainty at nominal load level

	Load model	P_{loss} (kW)	Deterministic	Lower	Upper
Without DG	CPL	Min	1.2562e-05	1.2184e-05	1.2940e-05
		Max	49.6749	47.8832	51.4904
		Mean	3.3059	3.1890	3.4242
		Std	8.3880	8.0892	8.6906
		CV	2.5373	2.5366	2.5380
With solar PV-DG	CPL	Min	1.2561e-05	1.2183e-05	1.2939e-05
		Max	15.0325	14.5640	15.5022
		Mean	1.2231	1.1847	1.2617
		Std	2.7308	2.6450	2.8169
		CV	2.2327	2.2326	2.2328
	CL	Min	1.2468e-05	1.2096e-05	1.2841e-05
		Max	12.4737	12.1515	12.7931
		Mean	1.0354	1.0077	1.0628
		Std	2.2805	2.2205	2.3401
		CV	2.2026	2.2018	2.2035

8. CONCLUSIONS

This paper proposes a probabilistic and possibilistic strategy to solve the power flow problem with optimally integrated solar PV-DG to investigate the impact of line and load uncertainties in the RDN. The N/w line and load vary in fixed and as function of Gaussian distribution, respectively. A new VSI is proposed to search the optimal site strategically for solar PV-DG to reduce power losses and enhance bus voltages. PSO method is further applied to determine the optimum solar PV-DG size. The independent method for finding the optimal site and size of the renewable DG provide openness and flexibility to the method. Two test cases have been designed and solved for varying levels of complexity in the PF problem. The bus voltage characteristic for various degree of belongingness is found to be affected by various realistic loads. The solution obtained from the proposed approach comprises all possible states of the N/w and converges faster than the existing results. The robustness of the method has been demonstrated on 33- and 69-bus N/w. It has been statistically approved from the analysis that the voltage profile and reduction in N/w power losses are under-represented for CPL model when compared to the CL model for all N/w loading conditions. The results imply that the proposed technique is more feasible and effective for the design of the large-scale N/w with a high degree of uncertainty. The narrower interval width signifies less conservative solution and numerical stability when compared to the FAA method. The findings revealed that uncertainties have a major impact on the RDN and so cannot be overlooked. A generalized set of equations for calculating N/w power losses with and without solar PV-DG considering uncertainties has been developed under various loading conditions which will help the DNOs in N/w planning and expansion of the RDN.

R<small>EFERENCES</small>

[1]   Noorkami et al., "Effect of temperature uncertainty on polymer electrolyte fuel cell performance", *International Journal of Hydrogen Energy*, vol. 39, no. 3, pp. 1439–1448, 2014.

[2]   Z. Wang and F.L. Alvarado, "Interval arithmetic in power flow analysis", *IEEE Transactions on Power* Systems, vol. 7, no. 3, pp. 1341–1349, 1992.

[3]   M. Aiena, M. Rashidinejad and M. Fotuhi-Firuzabad, "On possibilistic and probabilistic uncertainty assessment of power flow problem: A review and a new approach", *Renewable and Sustainable energy reviews*, vol. 37, pp. 883–895, 2014.

[4]   M.M. Aman, G.B. Jasmon, H. Mokhlis and A.H.A. Bakar, "Optimal placement and sizing of a DG based on a new power stability index and line losses", *International Journal of Electrical Power and Energy Systems*, vol. 43, no. 1, pp. 1296–1304, 2012.

[5]   L. Soo-Hyoung and P. Jung-Wook, "Selection of optimal location and size of multiple distributed generations by using Kalman Filter algorithm", *IEEE Transactions on Power System*, vol. 24, no. 3, pp. 1393–1400, 2009.

[6]   A.C. Rueda-Medina, J.F. Franco, M.J. Rider, A. Padilha-Feltrin and R. Romero, "A mixed integer linear programming approach for optimal type, size and allocation of distributed generation in radial distribution system", *Electric Power System Research*, vol. 97, pp. 133–143, 2013.

[7]   S.S. Parihar and N. Malik, "Optimal Allocation of Multi-Type DG in Radial Distribution System based on New Voltage Stability Index with Future Load Growth", *Evolving Systems*, pp. 1–15, 2020.

[8]   M. Mohsen, A.R. Youssef, M. Ebeed and S. Kamel, "Optimal Planning of Renewable Distributed Generation in Distribution Systems Using Grey Wolf Optimizer GWO", in Proceedings of the Nineteenth International Middle East Power Systems Conference, 2017, pp. 915–921.

[9]   S.S. Parihar and N. Malik, "Optimal allocation of renewable DGs in a radial distribution system based on new voltage stability index", *International Transaction on Electrical Energy System*, vol. 30, no. 4, pp. 1–19, 2020.

[10] S.S. Parihar and N. Malik, "Optimal allocation of multiple DGs in RDS using PSO & its impact on System Reliability", *Facta Universitatis, Series: Electronics and Energetics*, vol. 34, no. 2, pp. 219–237, 2021.

[11] E.S. Ali, S.M. Elazim and A.Y. Abdelaziz, "Ant lion optimization algorithm for renewable distributed generations", *Electrical Engineering*, vol. 100, no. 1, pp. 100–109, 2018.

[12] A.A. Hassan, F.H. Fahmy, A.E.S.A. Nafeh and M.A. Abu-elmagd, "Genetic single objective optimization for sizing and allocation of renewable DG systems", *International Journal of Sustainable Energy*, vol. 36, no. 6, pp. 545–562, 2017.

[13] B. Das, "Radial distribution power flow using interval arithmetic", *International Journal of Electrical Power and Energy Systems*, vol. 24, no. 10, pp. 827-836, 2002.

[14] P.M. Vidovic and A.T. Saric, "A novel correlated interval-based algorithm for distribution power flow calculation", *International Journal of Electrical Power and Energy Systems*, vol. 90, pp. 245–255, 2017.

[15] T. Ding, R. Bo, F. Li, Q. Guo, H. Sun, W. Gu and G. Zhou, "Interval power flow analysis using linear relaxation and optimality-based bounds tightening (OBBT) methods", *IEEE Transaction on Power System*, vol. 30, no. 1, pp. 177–188, 2015.

[16] A. Vaccaro, C.A. Canizares and D. Villacci, "An affine arithmetic-based methodology for reliable power flow analysis in the presence of data uncertainty", *IEEE Transactions on Power Systems, vol.* 25, no. 2, pp. 624–632, 2010.

[17] A. Chaturvedi, K. Prasad and R. Ranjan, "Use of interval arithmetic to incorporate the uncertainty of load demand for radial distribution system analysis", *IEEE Transactions on Power Delivery, vol.* 21, no. 2, pp. 1019–1021, 2006.

[18] S.S. Parihar and N. Malik, "Probabilistic Distribution based Interval Arithmetic Power Flow Analysis of Radial Distribution System with Distributed Generation and Composite Load Model", *Process integration and Optimization for sustainability*, pp. 1–13, 2021.

[19] B. Abdelkader, L. Slimani and T. Bouktir, "Analysis of radial distribution system power flow under uncertainties with fuzzy arithmetic algorithm", in Proceedings of the 3rd International Conference on Information Processing and Electrical Engineering, 2014.

[20] M. Esmaeili, M. Sedighizahed and M. Esmaili, "Multi-objective optimal reconfiguration and DG (Distributed Generation) power allocation in distribution networks using Big Bang-Big Crunch algorithm considering load uncertainty", *Energy*, vol. 103, pp. 86–99, 2016.

[21] M. Marin, F. Milano and D. Defour, "Midpoint-radius interval-based method to deal with uncertainty in power flow analysis", *Electric Power Systems Research*, vol. 147, pp. 81–87, 2017.

[22] G. Alefeld and J. Herzeberger, "Introduction to Interval Arithmetic", New York: Academic, 1983.

[23] M.E. El-Hawary and L.G. Dias, "Incorporation of load models in load flow studies. form of model effects", *IEE Proceedings C- Generation, Transmission and Distribution*, vol. 134, pp. 27–30, 1987.

[24] M.H. Haque, "Load flow solution of distribution systems with voltage dependent load models", *Electric Power and Systems Research*, vol. 36, pp. 151–156, 1996.

[25] K. Nagaraju, S. Sivanagaraju, T. Ramana and P.V. Prasad, "A Novel Load Flow Method for Radial Distribution Systems for Realistic Loads", *Electric Power Components and Systems*, vol. 39, no. 2, pp. 128–141, 2011.

[26] 1547-2003-IEEE standard for interconnecting distributed resources with electric power systems, IEEE Standards, pp. 1–16, 2003.

[27] R.A. Walling, R. Saint, R.C. Dugan, J. Burke and L.A. Kojovic, "Summary of distributed resources impact on power delivery systems", *IEEE Transaction on Power Delivery*, vol. 23, no. 3, pp. 1636–1644, 2008.

[28] J.H. Teng, "A direct approach for distribution system power flow solution", *IEEE Transactions on Power Delivery*, vol. 18, no. 3, pp. 882–887, 2003.

[29] V.V.S.N. Murty and A. Kumar, "Optimal placement of DG in radial distribution systems based on new voltage stability index under load growth", *International Journal of Electrical Power and Energy Systems*, vol. 69, pp. 246–256, 2015.

[30] M.E. Baran and F.F. Wu, "Network reconfiguration in distribution systems for loss reduction and load balancing", *IEEE Transactions on Power Delivery*, vol. 4, no. 2, pp. 1401–1407, 1989.

[31] R. Ranjan, B. Venkatesh and D. Das, "Voltage Stability Analysis of Radial Distribution Networks", *Electric Power Components and Systems*, vol. 31, pp. 501–511, 2003.

[32] R. Ishak, A. Mohamed, A.N. Abdalla and M.Z.C. Wanik, "Optimal placement and sizing of distributed generators based on a novel MPSI index", *International Journal of Electrical Power and Energy Systems*, vol. 60, pp. 389–398, 2014.

[33] S. Kansal, V. Kumar and B. Tyagi, "Hybrid approach for optimal placement of multiple DGs of multiple types in distribution networks", *International Journal of Electrical Power and Energy Systems*, vol. 75, pp. 226-235, 2016.

[34] P.D.P. Reddy, V.C.V. Reddy and T.G. Manohar, "Optimal renewable resources placement in distribution networks by combined power loss index and Whale Optimization Algorithms", *Journal of Electrical Systems and Information Technology*, vol. 5, no. 2, pp.175–191, 2018.

[35] A.R. Sobieh, M. Mandour, E.M. Saied and M.M. Salama, "Optimal number size and location of distributed generation units in radial distribution systems using Grey Wolf optimizer", *International Electrical Engineering Journal*, vol. 7, no. 9, pp. 2367–2376, 2017.

[36] W.S. Tan, M.Y. Hassan, M.S. Majid and H.A. Rahman, "Allocation and sizing of DG using cuckoo search algorithm", *IEEE International Conference on Power and Energy*, pp. 133-138, 2012.

[37] A.Y. Abdelaziz, Y.G Hegazy, W. El-Khattam and M.M. Othman, "A multi-objective optimization for sizing and placement of voltage-controlled distributed generation using supervised big bang–big crunch method", *Electric Power Components and Systems*, vol. 43, no. 1, pp. 105–117, 2015.

[38] D.Q. Hung, N. Mithulananthan and R.C. Bansal, "Analytical strategies for renewable distributed generation integration considering energy loss minimization", *Applied Energy*, vol. 105, pp. 75–85, 2013.